Faraday Discussions

Accepted Manuscript

Faraday Discussions

Royal Society of Chemistry

ROYAL SOCIETY OF CHEMISTRY

www.rsc.org/faraday_d

Supramolecular Control of Organic p/n-Heterojunctions by Complementary Hydrogen Bonding

Hayden T. Black,[a] Huaping Lin,[a] Francine Bélanger-Gariépy[b] and Dmitrii F. Perepichka*[,a]

  a) Department of Chemistry and Centre for Self-Assembled Chemical Structures, McGill
     University, Montreal, Qc H3A 0B8, Canada. *e-mail: dmitrii.perepichka@mcgill.ca
  b) Département de Chimie, Université de Montréal, Montréal, H3T 1J4, Qc, Canada
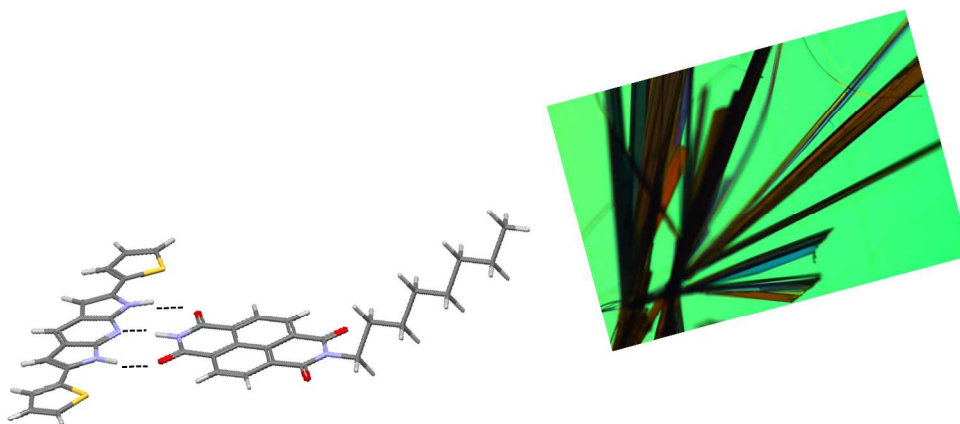
The supramolecular structure of organic semiconductors (OSCs) is the key parameter controlling their performance in organic electronic devices, and thus methods for controlling their self-assembly in the solid state are of outmost importance. Recently, we have demonstrated the co-assembly of p- and n-type organic semiconductors through a three-point hydrogen bonding interaction, utilizing an electron-rich dipyrrolopyridine (P2P) heterocycle which is complementary to naphthalenediimides (NDI) both in its electronic structure and H bonding motif. The H bonding mediated co-assembly between P2P donor and NDI acceptor leads to ambipolar co-crystals and provides unique structural control over their solid-state packing characteristics. In this paper we expand our discussion on the crystal engineering aspects of H bonded donor/acceptor assemblies, reporting three new single co-crystal x-ray diffraction structures and analyzing the different packing characteristics that arise from the molecular structures employed. Particular attention is given toward understanding the formation of the two general motifs observed, segregated and mixed stacks. Co-assembly of the donor and acceptor components into a single, crystalline material, allows the creation of ambipolar semiconductors where the mutual arrangement of p- and n-conductive channels is engineered by supramolecular design based on complementary H bonding.
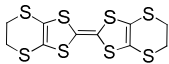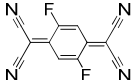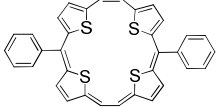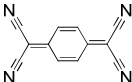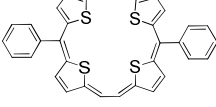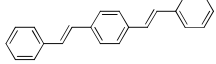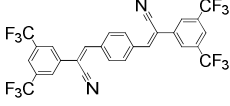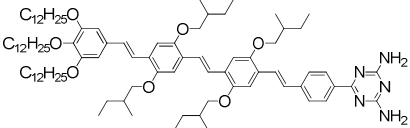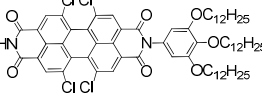
INTRODUCTION

Organic semiconductors (OSCs) possesses tunable molecular properties, accessible via the versatile tools of synthetic organic chemistry, and are therefore attractive electronic components for a variety of device applications. Structure-property relationships in OSCs enable, for example, band-gap engineering, control of redox properties, and tailoring of solubility. Thus, rational structural design and appropriate chemical substitution of OSCs has led to significant advancements in the performance of organic electronic devices. In organic photovoltaics (OPVs), band-gap engineering has led to improved solar absorption, providing increased short-circuit currents and enhanced power conversion efficiencies.[1] In organic field-

effect transistors (OFETs), control of the OSC frontier molecular orbital energies has enabled a tuning of the majority charge carrier, affording p-type, n-type, or ambipolar devices.[2]

In contrast to these molecular properties, the electrical properties of OSCs are intimately tied to the solid-state structure, which defines the efficiency of charge transport in specific directions.

Table 1. Reported donor/acceptor pairs used in co-assembly of bicomponent ambipolar semiconductors.

Donor	Acceptor	Packing motif	$^a\mu_h$ / $cm^2V^{-1}s^{-1}$	$^b\mu_e$ / $cm^2V^{-1}s^{-1}$	Ref
		mixed stack	$\sim 10^{-2}$	$\sim 10^{-2}$	3, 4
		mixed stack	4×10^{-2}	3×10^{-2}	5
		segregated stack	3×10^{-1}	1×10^{-2}	6
		mixed stack	7×10^{-3}	7×10^{-2}	7
		unknown	2×10^{-7}	2×10^{-7}	**Error! Bookmark not defined.**b

$^a\mu_h$ = hole mobility. $^b\mu_e$ = electron mobility.

Control of the solid-state structure requires a larger viewpoint than the conventional structure-property picture, which can only give insights into the isolated molecular properties (i.e. optical absorption, redox potentials, etc.). In order to truly control the electrical properties of OSCs, predictable intermolecular interactions are required in order to enable rational construction of desirable morphologies which are conducive to charge transport.

Highly ordered bicomponent OSCs prepared through co-crystallization of donor/acceptor components have recently emerged as an interesting class of optoelectronic materials (Table 1). In the realm of p/n organic heterojunctions, donor/acceptor co-crystals represent the ultimate case for long-range molecular ordering. Early strategies for co-crystallization relied on strong donor/acceptor components in order to facilitate π-orbital interactions, leading to a mixed stack solid-state arrangement of donor/acceptor components.[3,4,5] More recently, shape complementarity has been employed to help drive the co-crystallization of weaker donor/acceptor pairs. This approach has led to novel features in bi-component semiconductors, including segregated stack structures with balanced charge mobilities ~ 0.1 cm^2/Vs,[6] and luminescent ambipolar co-crystals.[7] While these materials have shown promising optoelectronic properties, the ability to fine tune the packing characteristics has been absent, since the co-

assembly of donor/acceptor through electronic or shape complementary interactions lacks directionality. New donor/acceptor co-crystal strategies which harness the predictive power of directed intermolecular interactions would greatly improve the structural control of these interesting electronic materials.

In recent years, hydrogen bonding (H bonding) has begun to emerge as a useful tool for manipulating the packing motifs of π-conjugated materials, and several studies have demonstrated efficient charge transport in OSCs possessing H bonding functionalities.[8] Notably, quinacridone based semiconductors with two-point self-complementary H bonding showed air-stable p-type OFETs with hole mobility as high as 1.5 cm^2/Vs, representing the best performance to date in organic transistors employing H bonding interactions.[8h] In other reports, self-complementary H bonding has been associated with a tighter packing in the crystal structure, resulting from the synergistic effects of H bonding and π-π interactions.[8b,d] Still, the incorporation of H bonding functionalities into OSCs has, for the most part, been unsystematic, mainly approached via empirical investigations of isolated material systems. The field of organic electronics would benefit from an improved understanding of the relationship between molecular structures with H bonding functionality, and their supramolecular organization in the solid state.

Compared to self-complementary interactions, H bonding between two complementary partners is attractive for electronic applications where more than one semiconductor component is required (i.e. for p/n heterojunctions). In the field of supramolecular chemistry, cross complementary H bonding stands as one of the most reliable interactions, and has been used for decades to construct a broad range of complex structures.[9] Self-assembly of DNA strands into the ubiquitous double-helix is perhaps most illustrative of the complexity and homogeneity obtainable through complementary H bonding, while the field of DNA nanotechnology[10] exemplifies the utility of complementary H bonding as a supramolecular synthon in materials science. In the field of organic metals, complementary H bonding has been explored for tuning both molecular packing and conductivity.[11,12] More recently, supramolecular ferroelectrics involving H bonding of electron donor and acceptor components, have been demonstrated.[13]

With the exception of only a few papers,[14] complementary H bonding between donor/acceptor OSCs remains largely unexplored. This is unfortunate, since the versatile intermolecular interaction could provide an effective handle for structural control of charge transport pathways in p/n heterojunctions. Early reports of complementary H bonding in donor/acceptor OSCs were limited to co-assemblies which lacked structural characterization, and therefore did not provide a clear picture as to what the role of H bonding was in dictating the solid-state organization. Nonetheless, complementary H bonding between an oligophenylene-vinylene/perylenediimide donor/acceptor pair afforded ambipolar thin-films, albeit with low charge mobilities of the order of 10^{-7} $cm^2V^{-1}s^{-1}$. **Error! Bookmark not defined.**[b]

Recently, we reported the co-crystallization of an electron donating diphenyl-dipyrrolopyridine (DP-P2P) with electron accepting naphthalenediimides (NDIs), mediated through a three-point complementary H bonding interaction (Scheme 1).[15] This approach led to crystalline materials with well-defined donor/acceptor interface controlled by the H bonding interaction, and solid-state packing characteristics that could be tuned via peripheral structural changes to the individual components. In this paper, we expand our investigation of the H bonding co-crystallization strategy, exploring new structural variants of both the P2P donors and NDI acceptors. Through analysis of the x-ray diffraction structures of six different donor/acceptor H bonded co-crystals, we offer insights into the relationship between the individual molecular structures employed and the resulting co-crystal packing characteristics. In addition, the charge transport properties of the individual components, as well as a selection of co-crystals, is examined through analysis of thin-film and single-crystal field effect transistor devices.
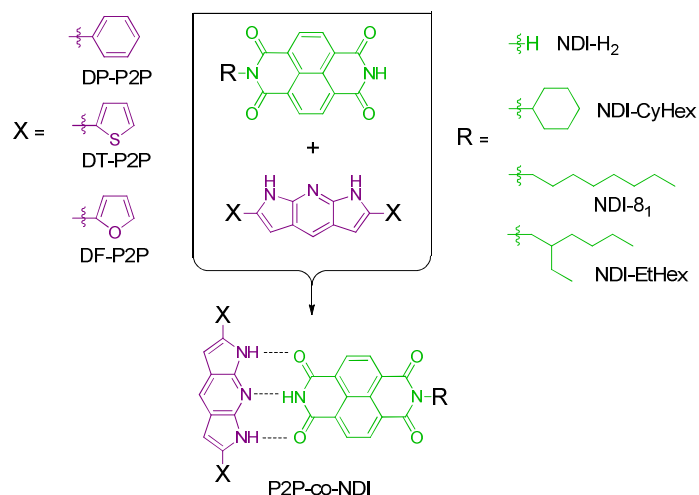
Scheme 1. P2P/NDI structures and their co-assembly.

EXPERIMENTAL SECTION

Materials and Methods. The syntheses of DP-P2P [16], NDI-8$_1$, and NDI-CyHex were carried out following previously published procedures.[15] The syntheses of DT-P2P, DF-P2P and NDI-EtHex will be published elsewhere. Co-crystals were grown via a two-step process, in which a stoichiometric mixture of P2P donor and NDI acceptor were first co-sublimed in a horizontal glass tube. The tube was evacuated at room temperature (~0.1 mbar) and then placed in a furnace with a hot zone at 340 °C and a crystallization zone at ~ 100 °C. The dark co-assembled powder was then removed from the tube and used as source material for the second stage growth, where physical vapor transport under a flow of either He or Ar (~ 50 mL/min) was performed with a hot zone at ~ 250 °C and crystallization zone near the exit of the furnace.

FET device fabrication. Single-crystal devices were fabricated as previously described.[15] Thin-film transistors were fabricated using a heavily n-doped Si wafer as gate electrode (Sb, resistivity = 0.005 – 0.025 ohm cm) with 200 nm SiOx as dielectric (capacitance = 17.2 nF/cm^2) and an octyl(trichloro)silane (OTS) monolayer. The hydrophobic OTS monolayer was first formed on the SiO$_x$ surface by submersion of the device substrate in a 0.1M OTS solution in toluene at 80 °C for 30 min. Thin-films of DP-P2P or NDI-8$_1$ were then deposited via vacuum sublimation at a rate of 0.1-0.2 Å/s, monitored using a quartz microbalance. Au source/drain electrodes (50 nm) were deposited through a shadow-mask via thermal evaporation at pressures < 5 × 10^{-6} torr. The I-V measurements on OFET devices were acquired under vacuum using a Keithley 4200-SCS semiconductor parameter analyzer.

DFT Calculations. All calculations were performed using B3LYP hybrid functional and 6-31G(d) basis set as implemented in Gaussian 09W.[17]

RESULTS AND DISCUSSION

Molecular Design of Complementary H bonding Donor/Acceptors

The design of electrically conducting supramolecular structures requires a careful selection of organic materials which meet the extensive requirements for semiconducting device applications. Specifically, we were focusing on identifying individual p/n components that combine the general materials requirements of OSCs, i.e. appropriate π-conjugation, suitable frontier molecular orbital energies, chemical and thermal stability, with high-fidelity supramolecular motifs, such as complementary H bonding. With this in mind, naphthalenediimide was chosen as a model n-type semiconductor component. It is one of the simplest and most chemically stable n-type organic materials which display sufficiently high electron mobility, often exceeding 0.1 cm^2/Vs.[18] It also offers a diverse structural space with properties that can be easily tuned through N-[19,20] and/or π-substitution,[21,22] and/or π-extension (as in perylene[23] and terrylene[24] homologues). More importantly, the unsubstituted imide functionality can act as a hydrogen acceptor-donor-acceptor (A-D-A) motif, engaging in high-fidelity H bonding interactions with molecules containing the complementary proton D-A-D functionality. 2,6-Diaminopyridine and its derivatives are among the most studied H bonding receptors.**Error! Bookmark not defined.**b[25,26] We reasoned that, utilizing this structural element in a fused dipyrrolo[2,3-b:3',2'-e]pyridine (P2P) heterocycle would lead to an ideal partner for co-assembly with NDIs because 1) it possesses the requisite complementary D-A-D motif and 2) the fused pyrrole rings impart an overall electron-rich character and rigid extended π-conjugated system, as required for efficient p-type semiconducting material.

Proceeding from our initial studies on the co-assembly of diphenyl-P2P (DP-P2P) with NDI[15], we explored structural variations with regards to the P2P peripheral aromatic substituents as well as the aliphatic N-substituents of NDI (Scheme 1). By replacing the phenyl substituents of DP-P2P with thienyl and furanyl groups, a stepwise increase in the electron donating character of the peripheral rings is achieved. This causes a progressive shift of the DFT calculated highest occupied molecular orbital (HOMO) energy to higher values, moving from -5.10 eV for DP-P2P to -4.91 eV for DF-P2P (Figure 1). The substitution also leads to crossover of the HOMO and HOMO-1 orbitals; the HOMO-1 of DP-P2P, which has an appearance typical of linearly conjugated polyaromatics, increases in energy and becomes the HOMO in DT-P2P and DF-P2P.
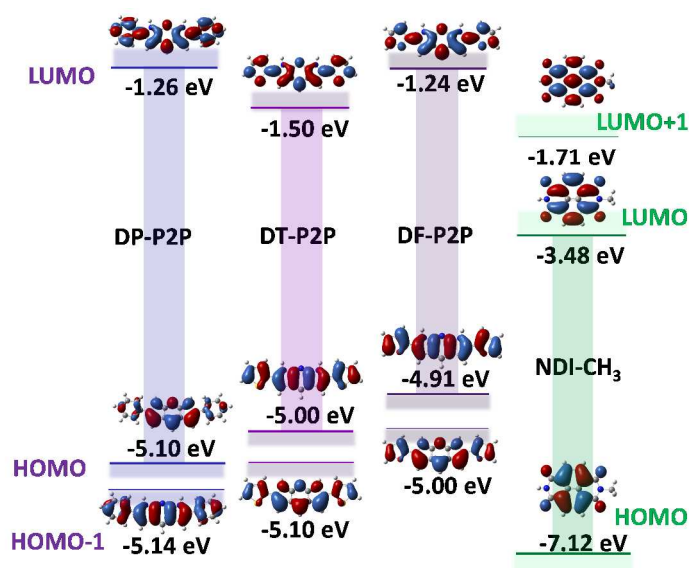
Figure 1. DFT calculated (B3LYP/6-31G(d)) frontier molecular orbital topologies and corresponding orbital energies of monoalkylated NDI-Me (green) and aryl-substituted P2P derivatives (purple).

Donor-acceptor interactions between NDI and P2P derivatives are manifested by the appearance of the new long-wavelength charge-transfer (CT) absorption band at ~500-700 nm, both in solution and in the solid state.[15] Also, while the studied NDI and P2P derivatives are highly fluorescent, both in solution and in the solid state, their H bonded complexes show no detectable emission, suggesting effective charge separation (photoinduced electron transfer) in these systems.

Single Co-Crystal X-Ray Diffraction Analysis

The growth of P2P/NDI single co-crystals was achieved via a two-step process as previously described for the DP-P2P-co-NDI derivatives.[15] First, the two components were mixed in powder form and co-sublimed under vacuum to form the complex under fast growth conditions. This step is necessary to ensure a stoichiometric vapor of the two components and obtain a high yield of the co-assembly, but leads to small crystals that are not suitable for x-ray diffraction. The co-crystal powder can then be used to grow larger single crystals of higher quality via a slow growth in a horizontal physical vapor transport process, using a flow of either He or Ar at ambient pressure. The black color of the co-crystals brought about by the charge-transfer interactions makes them distinctly different from the colorless individual donor/acceptor components, which facilitates optimization of the co-sublimation procedure.

The resulting co-crystals were analyzed using x-ray diffraction and, in some cases, single crystal transistor devices. The high-fidelity of the complementary H bonding provides a robust co-crystallization approach, tolerant to significant structural variations of each component. The single crystal x-ray diffraction data is collected in Table 2 for the six co-crystals discussed here, as well as for pure DP-P2P. In all cases the co-crystallization afforded a predictable donor/acceptor interface defined by the three-point complementary H bonding. Figure 2 shows the packing configurations for compounds DP-P2P-co-NDI-H_2 and DP-P2P-co-NDI-8_1, both of which form segregated stacks with isolated columns of donor and acceptor. This type of packing motif is rarely observed in donor/acceptor co-crystals,[6] which usually prefer to organize into mixed stacks in order to maximize π-π interactions between donors and acceptors.[3,5,7] The segregated stack motif is reminiscent of the ideal morphology for OPVs, where the alternation of donor/acceptor domains maximizes exciton dissociation and provides percolating channels for hole/electron transport. The stoichiometry of the p- and n-channel materials is precisely controlled by the molecular structure. Thus, removing the alkyl chain from NDI component liberates the second H bonding functionality and predictably leads to 2:1 stoichiometry in the DP-P2P-co-NDI-H_2 cocrystals.

It should be noted that despite the segregation of donor and acceptors into separated p- and n-domains, donor/acceptor interactions are still observed (Figure 2c, red dotted lines). Although the π-π overlap is small, the donor….acceptor contacts in these segregated stack structures are even shorter than those in the mixed stack structures discussed below. This is likely due to weaker steric repulsion between the donor/acceptor molecules, which are significantly slipped from co-facial arrangement. At the same time, this π-π interaction between DP-P2P and NDI polarizes DP-P2P, and the introduced Coulombic repulsion increases the separation of the DP-P2P molecules within the herringbone columns ($d_{P2P\ \pi-CH}$, Table2).
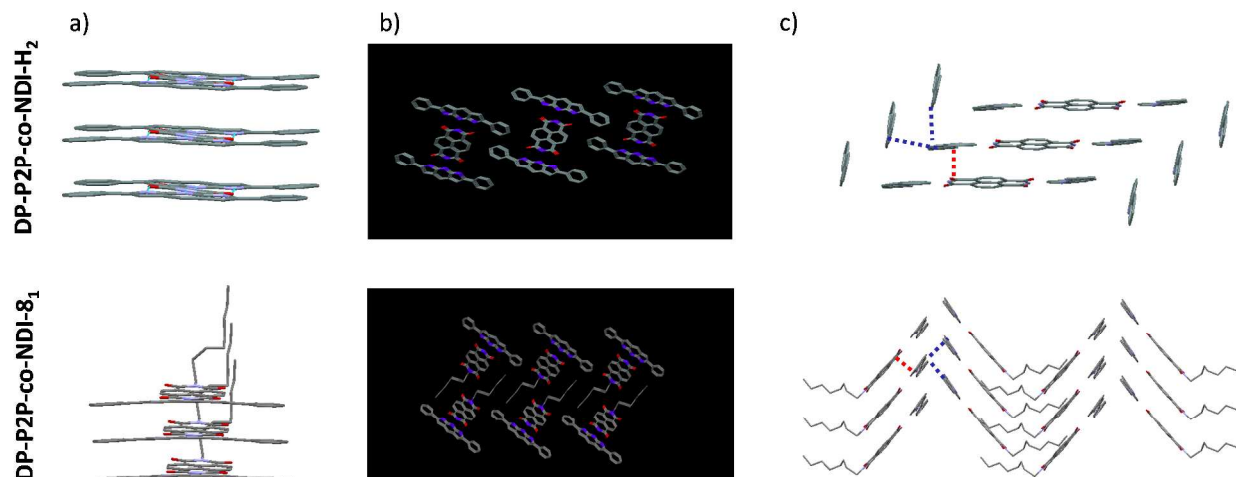
Figure 2. Single co-crystal x-ray diffraction structures for segregated stacks DP-P2P-co-NDI-H_2 and DP-P2P-co-NDI-8_1, with slices depicting a) π-π stacking, b) columnar arrangement of π stacks, and c) lateral herringbone organization. Dotted blue and red lines show the shortest $\pi\ldots\pi$ contacts between the donor molecules and between the donor and acceptor, respectively.

Table 2. Single-crystal x-ray diffraction data (Å).

| Crystal	Packing Motif	a / Å (α / °)	b / Å (β / °)	c / Å (γ / °)	$d_{\text{H-bonding}}$ O-H / Å	$d_{\text{H-bonding}}$ N-H / Å	$^a d_{\text{P2P/NDI }\pi\text{-}\pi}$ C-C / Å	$^b d_{\text{P2P/P2P}}$ C-C / Å	$^c d_{\text{NDI/NDI}}$ C-C / Å
DP-P2P	herring-bone	11.20 (90.0°)	7.22 (91.0°)	18.25 (90.0°)	N/A	2.22, 2.16	N/A	3.43	N/A
DP-P2P-co-NDI-H_2	segregated stack	18.83 (90.0°)	5.11 (91.9°)	21.29 (90.0°)	2.13, 1.96	1.82	3.05	3.59	3.30
DP-P2P-co-NDI-8_1	segregated stack	14.50 (90.0°)	5.11 (104.2°)	23.00 (90.0°)	2.26, 2.08	1.91	3.13	3.43	3.41
DP-P2P-co-NDI-CyHex	mixed stack	6.91 (96.4°)	13.00 (94.9°)	19.43 (97.2°)	2.24, 2.14	1.95	3.17	4.32	3.48
DT-P2P-co-NDI-EtHex	mixed stack	6.93 (88.6°)	13.34 (84.2°)	18.51 (76.7°)	2.16, 2.13	1.95	3.22	4.33	3.33
DF-P2P-co-NDI-8_1	mixed stack	22.00 (90.0°)	9.38 (106.0°)	31.70 (90.0°)	2.24, 2.15 (2.30, 2.05)	1.96 (1.94)	3.17	7.47	3.25
DF-P2P-co-NDI-CyHex	mixed stack	17.94 (90.0°)	9.35 (112.6°)	19.47 (90.0°)	2.24, 2.09	1.94	3.26	7.05	3.25

^{a}Shortest intermolecular P2P/NDI C-C distance. ^{b}Shortest intermolecular P2P/P2P C-C distance. ^{c}Shortest intermolecular NDI/NDI C-C distance.

Upon transition from the linear octyl substituent in DP-P2P-co-NDI-8$_1$ to the cyclohexyl substituent in DP-P2P-co-NDI-CyHex, a shift from segregated stack to mixed stack is observed. This can be explained by the steric effect of the cyclohexyl ring, which protrudes out of the π-orbital plane and prohibits co-facial approach of two NDI molecules (Figure 3c). In this alternating donor/acceptor arrangement the NDI-CyHex settles slightly off-center from the core of DP-P2P, with several short contacts between the electron deficient naphthalene and the electron rich dipyrrolopyridine. A 40.5° twist of one peripheral phenyl group limits the π-conjugation within the DP-P2P molecules, but at the same time it allows secondary π-interactions between the phenyl rings in adjacent columns. Thus, the π-stacks are separated by regions of interacting phenyl rings and are arranged into parallel, co-planar columns.

An almost identical packing is observed in the DT-P2P-co-NDI-EtHex co-crystal, with alternating donor/acceptor π-π interactions giving rise to mixed stack columns, separated by regions of interacting thiophene rings. Steric repulsion of the branched N-ethylhexyl substituent could again be responsible for alternating stacking in DT-P2P-co-NDI-EtHex, reiterating the importance of the N-substituent on NDI. Both thiophene rings are twisted out of plane by ~ 30° in order to accommodate the mentioned above secondary π-interactions.

When strongly electron-donating furan rings are employed in the co-crystal DF-P2P-co-NDI-8$_1$, a mixed stack arrangement is obtained, even with the sterically uninhibiting octyl substituent on the NDI component. The location of the donor/acceptor π-π overlap is shifted away from the P2P core and closer to the more electron rich furan-containing periphery (Figure 3a). In contrast to DP-P2P and DT-P2P derivatives, the peripheral furan rings are almost perfectly planar with respect to the P2P core (3-11°). The increased planarity of oligofurans (compared with oligothiophenes) has previously been noted and explained by the reduced steric repulsions (due to the smaller oxygen atom) and lower aromaticity of furan, which increases interring electron delocalization, enhancing the quinoidal character.[27] As a result of the planar DF-P2P structures in these co-crystals, the above mentioned secondary π-interactions of terminal rings, observed for DP-P2P and DT-P2P co-crystals are not favored. In order to maximize the interaction between the π-columns, they pack in a 'herringbone- like' pattern, where the aromatic planes of the molecules from adjacent columns are not co-parallel (Figure 3b).
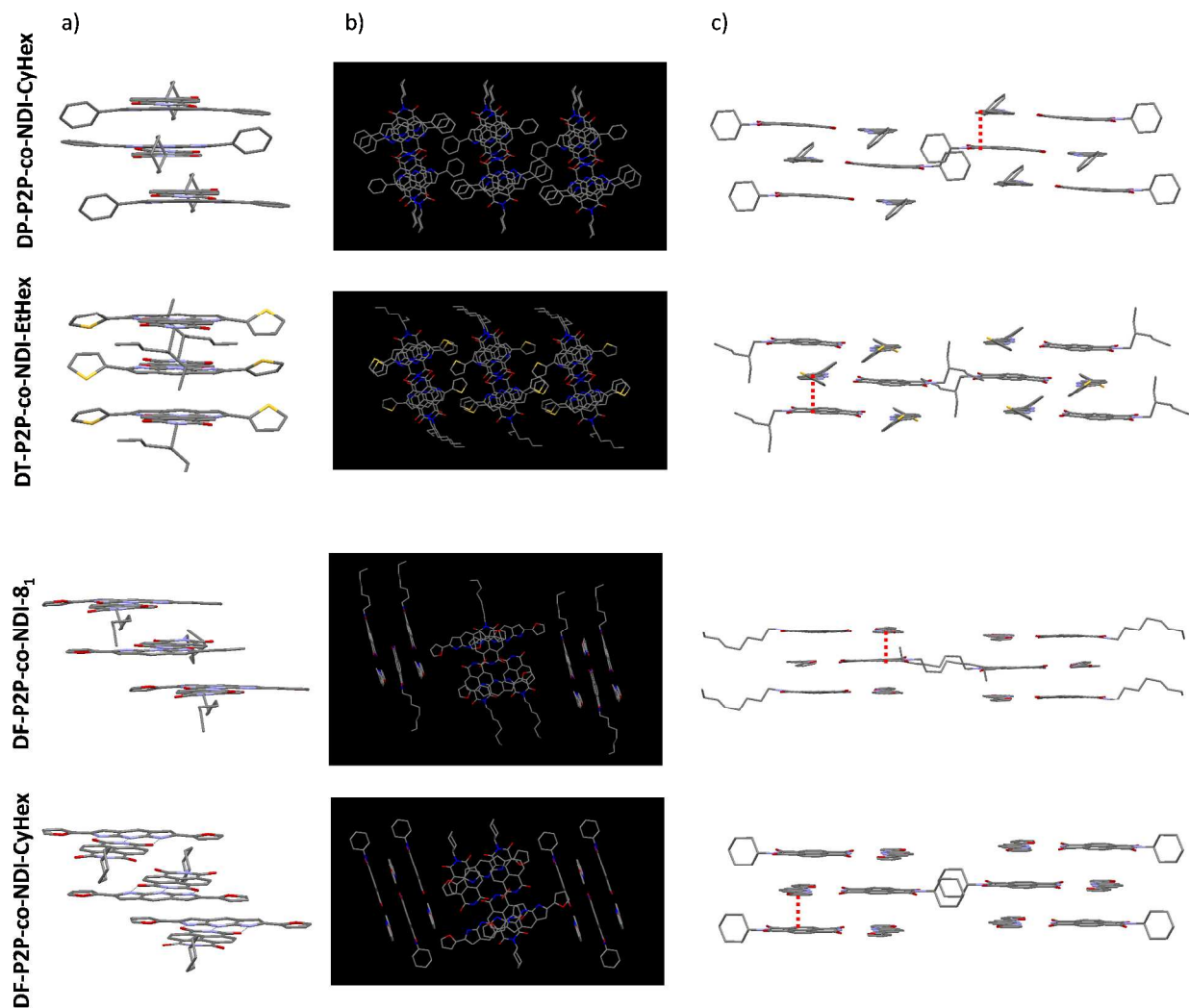
Figure 3. Single co-crystal x-ray diffraction structures for mixed stacks DP-P2P-co-NDI-CyHex, DT-P2P-co-NDI-EtHex, DF-P2P-co-NDI-8$_1$ and DF-P2P-co-NDI-CyHex, with slices depicting a) π-π stacking, b) the columnar arrangement of π stacks, and c) the lateral organization of mixed stack columns.

Together, these six co-crystals enable the formulation of design rules for the rational construction of desirable donor/acceptor supramolecular structures. While a mixed stack organization does not necessarily preclude efficient charge transport (see discussion below), the segregated stacks are potentially of greater interest for semiconducting device applications, since clear hole/electron transporting channels can be identified in these structures, and because segregated stacks are more likely to maintain the electronic properties of the individual semiconductor components. It is first noted that only co-crystals using DP-P2P as donor showed segregated stack organization, while those incorporating DT-P2P and DF-P2P all displayed a mixed stack. This can in part be explained by the electronic structure of the three donors; DP-P2P is the weakest donor with HOMO level at -5.1 eV, and therefore possesses weaker donor/acceptor interactions (which favor co-facial mixed stacking). Thus, while DP-P2P-co-NDI-8$_1$ shows a segregated stack, the stronger donor characteristic of DF-P2P affords a mixed stack arrangement in DF-P2P-co-NDI-8$_1$. A second important consideration arises from the steric constraints,

as evidenced by the shift to a mixed stack arrangement for DP-P2P-co-NDI-CyHex. In order to promote segregated stacks one must also ensure the facile approach of donor-to-donor and acceptor-to-acceptor.
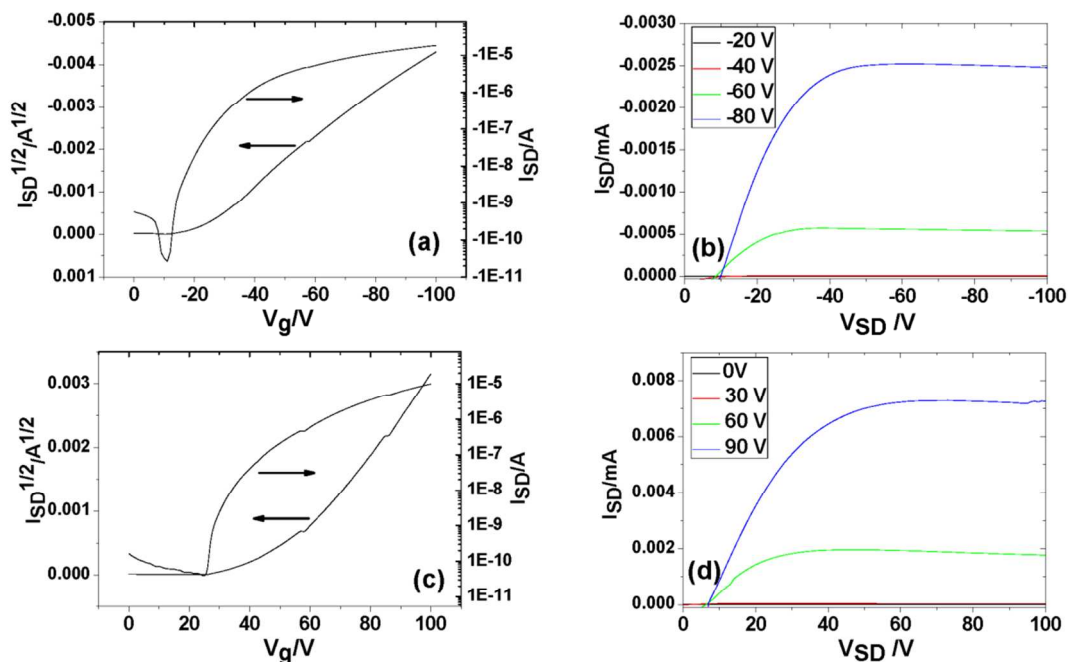
Figure 4. Thin-film transistor transfer (a, c) and output (b, d) characteristics for DP-P2P (a,b) and NDI-8_1 (c,d).

Charge Transport Properties of Individual Components and their Co-Assemblies

The hole and electron transport properties of DP-P2P and NDI derivatives were investigated using OFET devices. Device studies were focused only on DP-P2P as the p-type component, for which co-crystals containing both segregated and mixed stacks were obtained. Thin-film transistors (TFT) were fabricated for DP-P2P and NDI-8_1 using Si(n++)/SiO$_x$ as gate electrode and dielectric, respectively, employing a hydrophobic self-assembled monolayer by reaction of the silanol surface groups with octyltrichlorosilane. The TFT device characteristics are summarized in Table 3 and the I-V curves are shown in Figure 4. The DP-P2P transistors displayed typical p-type (only) characteristics with good saturation behavior. The devices afforded an average hole mobility (calculated from saturation regime) of $\mu_h = 0.045$ cm^2/Vs, with relatively low threshold voltage $V_T = -10$V and on/off current ratios reaching $I_{on/off} = 10^5$. The NDI-8_1 TFT devices showed only an n-type response, with an electron mobility of $\mu_e = 0.047$ cm^2/Vs, higher threshold voltage of $V_T = 40$V, and $I_{on/off} = 10^5$. Such balanced hole and electron-transport characteristics of DP-P2P and NDI-8_1 makes them the ideal pair to explore the co-assembly of p/n heterojunctions. It is also important to note that the presence of acidic (imide, pKa <10) and basic (pyridine, pKa >5) functional groups in these materials does not appear detrimental for efficient hole/electron transport, which is an important pre-requisite for using H bonding in design of semiconducting materials. Indeed, dialkylated NDI-8_2 which possesses very similar electronic properties and similar herringbone packing in the solid state, but lacks the H bonding functionality of NDI-8_1, displays a similar electron mobility (0.16 cm^2/Vs) in thin film OFET devices.[28] Although some examples of efficient charge transport in the presence of

weakly acidic functionalities (NH) has been reported before,[8b,c,e,f,g,h] these are typically avoided in the design of an OSC due to concerns of charge trapping via protonation/deprotonation of charge carriers.[2]

Note, that compared to the thin-film devices, single-crystal transistors showed a decrease in hole mobility for DP-P2P by a factor of ~2, whereas NDI-8_1 single-crystal devices showed an improvement in electron mobility by a factor of ~2. The inconsistent trend in going from thin-film to single-crystal device architecture reflects the balance of two effects; the increased molecular order/eliminated grain boundaries in single crystal device improves the charge transport within the channel, while the relatively high semiconductor thickness (which is difficult to control in single crystal device) increases the contact resistance in these top-contact device, suppressing charge injection. Nevertheless, single crystal OFETs have been chosen to explore the co-assembled semiconducting materials, as it eliminates the uncertainty of the composition and structure of the bottom-most layer of the semiconducting channel.

Table 3. Thin-film and single crystal field-effect transistor properties of individual components and co-crystals

Semiconductor	$^{a}\mu_h$ (cm^2/Vs)	$^{a}\mu_e$ (cm^2/Vs)	$^{b}V_T$ (V) (hole/electron)	$^{c}I_{on/off}$ (hole/electron)
TFT Devices				
DP-P2P	0.045	-	-10/ -	10^5
NDI-8_1	-	0.047	- / 40	10^5
Single Crystal Devices				
DP-P2P	0.027	-	-15/ -	10^4 / -
NDI-8_1	-	0.081	- / 35	- / 10^5
NDI-CyHex	-	0.17	- / 20	- / 10^5
DP-P2P-co-NDI-H$_2$	-	0.00034	- / 7	- / 10^2
DP-P2P-co-NDI-8_1	0.043	0.089	-94 / 7	10^1 / 10^3
DP-P2P-co-NDI-CyHex	0.00041	0.22	-71 / 4	10^3 / 10^6

$^{a}\mu_h$ *and* μ_h are the field-effect hole and electron mobilities, respectively (measured in saturated regime). $^{b}V_T$ is the threshold voltage. $^{c}I_{on/off}$ is the ratio of the maximum to minimum I_{SD}, obtained from the transfer characteristics.

All of the co-assemblies employing DP-P2P exhibited a field-effect response in single-crystal devices, as previously reported.[15] While the DP-P2P-co-NDI-H$_2$ co-crystal only showed n-type behavior with low electron mobility of μ_e = 0.00034 cm^2/Vs, both DP-P2P-co-NDI-8_1 and DP-P2P-co-NDI-CyHex demonstrated ambipolar transport. The DP-P2P-co-NDI-8_1 featuring segregated stacks in its crystal structure, afforded balanced hole and electron mobilities (μ_h = 0.043 cm^2/Vs and μ_e = 0.089 cm^2/Vs), which are very similar to the values obtained for the individual components. Efficient hole transport in DP-P2P-co-NDI-8_1 can be related to the tight herringbone packing of P2P molecules, with the shortest P2P/P2P C-C contact (3.43Å) identical to that in pure DP-P2P. On the other hand, DP-P2P-co-NDI-CyHex afforded the highest electron mobility of μ_e = 0.22 cm^2/Vs, but gave a lower hole mobility of μ_h = 0.00041 cm^2/Vs. Although such a large difference in electron and hole transporting properties is not desirable for most device applications, it is remarkable that a rather high electron mobility was achieved for a mixed stack architecture, with no continuous π-interactions between the NDI molecules. This could potentially be explained by superexchange mechanism (involving π-orbitals of the donor DP-P2P

component).[29] In fact, moderately high charge mobility in mixed stack cocrystals has been reported before (Table 1).

The unique character of each studied single-crystal (i.e. thickness, surface roughness) and manual device assembly process limits the reproducibility of single-crystal device studies, and the data does not provide a statistical measure of each co-assembly's electrical properties. On the other hand, important information is gained from these experiments, such as the confirmation of ambipolar transport in both segregated and mixed stack co-crystal structures. Furthermore, the complementary H bonding interaction does not compromise the electrical performance of the individual components, as observed in DP-P2P-co-NDI-8_1 which supported hole and electron mobilities as high as the best performing devices from the pure materials. These results demonstrate the ability to construct bicomponent, crystalline donor/acceptor structures through predictable H bonding interactions, leading to electrically functional ambipolar p/n molecular heterojunctions.


Conclusions and Outlook

By taking advantage of the high-fidelity complementary A-D-A….D-A-D H bonding motif, we have demonstrated rational molecular-level design of donor/acceptor co-crystals. Crystallographic analysis of six different H bonded donor/acceptor co-crystals has revealed the relationships which link the individual donor/acceptor structures with their supramolecular organization. Segregated stack structures were observed in two co-crystals, arising from the co-assembly of relatively weak donor/acceptor pairs that possess molecular structures which are compatible with self-aggregation after H bonding complexation. On the other hand, mixed stack structures are obtained when the donor/acceptor electronic interaction is stronger, or when the steric hindrance imposed by substituents prevents packing via self-aggregation of the donor and acceptor.

Field-effect transistor studies, performed in thin film and single crystal devices, show that the presence of acidic (NH) and basic (pyridine) functionalities in the H bonding components, generally thought of as charge trapping centers, is not detrimental to either electron or hole mobility. Co-crystallization of the donor P2P and acceptor NDI components creates an ambipolar materials with the electron and hole mobilities resembling those in individual components.

One of the goals for our lab in moving forward with H bonding mediated co-assembly of donor/acceptors is to fabricate supramolecular structures with photovoltaic properties. For OPV applications, a large p/n interfacial area is required for efficient exciton dissociation, a feature that is omnipresent in P2P/NDI co-crystals. Indeed, complete quenching of the fluorescence of individual components in the coassembled materials indicates an efficient exciton dissociation by an electron transfer from the donor to the acceptor. On the other hand, efficient OPV heterojunctions require spatial separation of hole/electron pairs in order to enhance charge collection and reduce charge recombination. For this reason, most bulk heterojunction OPVs feature p-/n-domain sizes of the order of 10-50 nm. This presents a problem for molecular heterojunction co-crystals, where the domain size cannot easily be tuned. One method for circumventing the problem of hole/electron proximity in donor/acceptor co-crystals is to construct a molecularly defined p/n interface possessing a redox gradient, which would shuttle holes and electrons away from the p/n interface after exciton dissociation (Figure 5). In order to accomplish this using the P2P-NDI H bonded interface, a stronger electron donor (lower oxidation potential than P2P) would be covalently linked to P2P, while a strong electron acceptor (lower reduction potential than NDI) would be linked to NDI. This type of system would mimic certain aspects of the

highly efficient supramolecular complexes involved in photosynthesis. One can also imagine the implementation of this concept (as well as P2P and NDI building blocks) in designing donor and acceptor semiconducting polymers/long chain oligomers, where the phase separation will be controlled by complementary H bonding between the donor and acceptor strands.
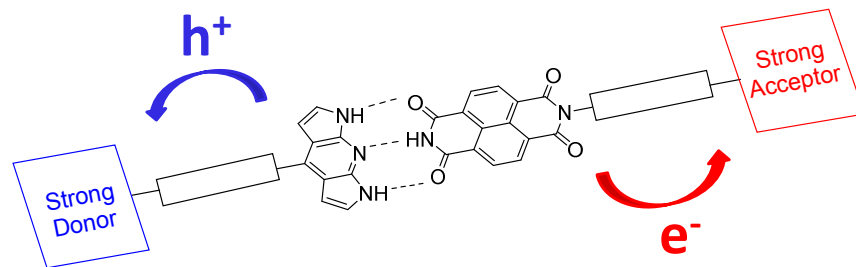
Figure 5. Proposed P2P-NDI H bonded co-assembly capable of effective charge separation.

In conclusion, the prospects of using complementary H bonding to control the supramolecular organization of electronic materials are immense, and H bonding is perhaps the most versatile and reliable route towards solid-state structural control in organic electronics.

Additional Information. Crystallographic files of the discussed structures DP-P2P (990667), DP-P2P-*co*-NDI-8₁ (990641), DP-P2P-*co*-NDI-H₂ (990642), DP-P2P-*co*-NDI-CyHex (990643), DT-P2P-*co*-NDI-EtHex (1008322), DF-P2P-*co*-NDI-8 (1008323) and DF-P2P-*co*-NDI-CyHex (1008324) can be obtained from CCDC.

References

[1] H. Zhou, L. Yang and W. You, *Macromolecules* **2012**, *45*, 607.

[2] a) A. R. Murphy and J. M. J. Fréchet *Chem. Rev.* **2007**, *107*, 1066. (b) S. Z. Bisri, C. Piliego, J. Gao and M. A. Loi, Adv. Mater. **2014**, *26*, 1176.

[3] T. Hasegawa, S. Kagoshima, T. Mochida, S. Sugiura and Y. Iwasa, *Solid State Commun.* **1997**, *103*, 489.

[4] M. Sakai, H. Sakuma,Y. Ito, A. Saito, M. Nakamura, K. Kudo, *Phys. Rev. B* **2007**, *76*, 045111.

[5] J. Zhang, H. Geng, T. Singh Virk, Y. Zhao, J. Tan, C. Di, W. Xu, K. Singh, W. Hu, Z. Shuai, Y. Liu and D. Zhu, *Adv. Mater.* **2012**, *24*, 2603.

[6] J. Zhang, J. Tan, Z. Ma, W. Xu, G. Zhao, H. Geng, C. Di, W. Hu, Z. Shuai, K. Singh and D. Zhu, *J. Am. Chem. Soc.* **2013**, *135*, 558.

[7] S. K. Park, S. Varghese, J. H. Kim, S.-J. Yoon, O. K. Kwon, B.-K. An, J. Gierschner and S. Y. Park, *J. Am. Chem. Soc.* **2013**, *135*, 4757.

[8] a) H.-L. Yip, H. Ma, A. K.-Y. Jen, J. Dong and B. A. Parviz, *J. Am. Chem. Soc.* **2006**, *128*, 5672. b) M. Gsänger, J. H. Oh, M. Könemann, H. W. Höffken, A.-M. Krause, Z. Bao and F. Würthner, *Angew. Chem. Int. Ed.* **2010**, *49*, 740. c) J. A. Oh, W.-Y. Lee, T. Noe, W.-C. Chen, M. Könemann and Z. Bao, *J. Am. Chem. Soc.* **2011**, *133*, 4204. d) Z. He, D. Liu, R. Mao, Q. Tang and Q. Miao, *Org Lett.* **2012**, *14*, 1050. e) Y. Suna, J. Nishida, Y. Fujisaki and Y. Yamashita, *Org. Lett.* **2012**, *14*, 3356. f) N. B. Kolhe, R. N. Devi, S. P. Senanayak, B. Jancy, K. S. Narayan and S. K. Asha, *J. Mater. Chem.* **2012**, *22*, 15235. g) E. D. Głowacki, L. Leonat, M. Irimia-Vladu, R. Schwödiauer, M. Ullah, H. Sitter, S. Bauer and N. S. Sariciftci, *Appl. Phys. Lett.* **2012**, *101*, 023305. h) E. D. Głowacki, M. Irimia-Vladu, M. Kaltenbrunner, J. Gsiorowski, M. S. White, U. Monkowius, G. Romanazzi, G. P. Suranna, P. Mastrorilli, T. Sekitani, S. Bauer, T. Someya, L. Torsi and N. S. Sariciftci, *Adv. Mater.* **2013**, *25*, 1563.

[9] L. J. Prins, D. N. Reinhoudt and P. Timmerman, *Angew. Chem. Int. Ed.* **2001**, *40*, 2382.

[10] F.A. Aldaye, A. L. Palmer and H. F. Sleiman, *Science* **2008***, 321*, 1795.

[11] M. Fourmigué and P. Batail, *Chem. Rev.* **2004**, *104*, 5379.

[12] T. Murata, Y. Morita, Y. Yakiyama, K. Fukui, H. Yamochi, G. Saito and K. Nakasuji, *et al. J. Am. Chem. Soc.* **2007**, *129*, 10837.

[13] A. S. Tayi, A. K. Shveyd, A. C.-H. Sue, J. M. Szarko, B. S. Rolczynksi, D. Cao, T. J. Kennedy, A. A. Sarjeant, C. L. Stern, W. F. Paxton, W. Wu, S. K. Dey, A. C. Fahrenbach, J. R. Guest, H. Mohseni, L. X. Chen, K. L. Wang, J. F. Stoddart, S. L. Stupp, *Nature* **2012**, *488*, 485.

[14] a) C.-H. Huang, N. D. McClenaghan, A. Kuhn, J. W. Hofstraat, D. M Bassani, *Org. Lett.* **2005**, *7*, 3409. (b) P. Jonkheijm, N. Stutzmann, Z. Chen, D. M. de Leeuw, E.W. Meijer, A. P. H. J. Schenning and F. Würthner, *J. Am. Chem. Soc.* **2006**, *128*, 9535.

[15] H. T. Black and D. F. Perepichka, *Angew. Chem. Int. Ed.* **2014**, *53*, 2138.

[16] C. Koradin, W. Dohle, A. L. Rodriguez, B. Schmid and P. Knochel *Tetrahedron* **2003**, *59*, 1571

[17] Frisch, M. J.; Trucks, G. W.; Schlegel, H. B.; Scuseria, G. E.; Robb, M. A.; Cheeseman, J. R.; Scalmani, G.; Barone, V.; Mennucci, B.; Petersson, G. A.; Nakatsuji, H.; Caricato, M.; Li, X.; Hratchian, H. P.; Izmaylov, A. F.; Bloino, J.; Zheng, G.; Sonnenberg, J. L.; Hada, M.; Ehara, M.; Toyota, K.; Fukuda, R.; Hasegawa, J.; Ishida, M.; Nakajima, T.; Honda, Y.; Kitao, O.; Nakai, H.; Vreven, T.; Montgomery, J. A.; Peralta, J. E.; Ogliaro, F.; Bearpark, M.; Heyd, J. J.; Brothers, E.; Kudin, K. N.; Staroverov, V. N.; Kobayashi, R.; Normand, J.; Raghavachari, K.; Rendell, A.; Burant, J. C.; Iyengar, S. S.; Tomasi, J.; Cossi, M.; Rega, N.; Millam, J. M.; Klene, M.; Knox, J. E.; Cross, J. B.; Bakken, V.; Adamo, C.; Jaramillo, J.; Gomperts, R.; Stratmann, R. E.; Yazyev, O.; Austin, A. J.; Cammi, R.; Pomelli, C.; Ochterski, J. W.; Martin, R. L.; Morokuma, K.; Zakrzewski, V. G.; Voth, G. A.; Salvador, P.; Dannenberg, J. J.; Dapprich, S.; Daniels, A. D.; Farkas; Foresman, J. B.; Ortiz, J. V; Cioslowski, J.; Fox, D. J. Gaussian 09, Revision B.01, *Gaussian, Inc., Wallingford CT* **2009**.

[18] a) B. A. Jones, A. Facchetti, T. J. Marks and M. R. Wasielewski, *Chem. Mater.* **2007**, *19*, 2703. b) D. Shukla, S. F. Nelson, D. C. Freeman, M. Rajeswaran,W. G. Ahearn, D. M. Meyer and J. T. Carey, *Chem. Mater.* **2008**, *20*, 7486. c) K. C. See, C. Landis, A. Sarjeant and H. E. Katz, *Chem. Mater.* **2008**, *20*, 3609.

[19] H. E. Katz, J. Johnson, A. J. Lovinger and W. Li, *J. Am. Chem. Soc.* **2000**, *122*, 7787.

[20] R. Schmidt, J. H. Oh, Y.-S. Sun, M. Deppisch, A.-M. Krause, K. Radacki, H. Braunschweig, M. Könemann, P. Erk, Z. Bao and F. Würthner, *J. Am. Chem. Soc.* **2009**, *131*, 6215.

[21] Y. Zhao, C. Di, X. Gao, Y. Hu, Y. Guo, L. Zhang, Y. Liu, J. Wang, W. Hu, and D. Zhu, *Adv. Mater.* **2011**, *23*, 2448.

[22] B. A. Jones, A. Facchetti, M. R. Wasielewski and T. J. Marks, *J. Am Chem. Soc.* **2007**, *129*, 15259.

[23] C. Li and H. Wonneberger, *Adv. Mater.* **24**, 613-636 (2012).

[24] J. H. Oh, W.-Y. Lee, T. Noe, W.-C. Chen, M. Könemann and Z. Bao, *J. Am. Chem. Soc.* **2011**, *133*, 4204

[25] S.-K. Chang, D. V. Engen, E. Fan, A. D. Hamilton, *J. Am. Chem. Soc*. **1991**, *113*, 7640.

[26] M. Gray, A. O. Cuello, G. Cooke, V. M. Rotello, *J. Am. Chem. Soc*. **2003**, *125*, 7882,

[27] Gidron, O.; Bendikov, M. *Angew. Chem. Int. Ed*. **2014**, *53*, 2546.

[28] H. E. Katz, J. Johnson, A. J. Lovinger and W. Li, *J. Am. Chem. Soc*. **2000**, *122*, 7787

[29] L. Zhu, Y. Yi, Y. Li, E.-G. Kim, V. Coropoceanu, J.-L. Brédas, *J. Am. Chem. Soc*. **2012**, *134*, 2340